from Chemistry and Physics of Solid Surfaces IV, R. Vanselow and R. Howe, eds. (Springer, Berlin, Heidelberg, New York, 1982)

11. Critical Phenomena of Chemisorbed Overlayers

T.L. Einstein

With 8 Figures.

11.1 Introduction

Critical phenomena refer to the singular behavior of various thermodynamic properties, particularly the divergence of the size of fluctuations near second-order phase transitions. This behavior has surprisingly little to do with the microscopic Hamiltonian describing the system or the species undergoing the phase change; instead, it is determined by the dimensionality of the system and the symmetry of the ordered state. Based on these attributes, transitions can be classified into a small number of universality classes. All members of such a class have common critical exponents which describe the singularities near the transition. The dependence on spatial dimensionality d is quite strong. For d = 1, fluctuations are so strong that long-range order is impossible (except when long-range forces are present). In fact, for a pure 2-d system, long-range order as conventionally defined is, in principal, also impossible (two recent reviews are [11.1]), although in realistic experimental systems these limitations enter only weakly. On the other hand, similar considerations lead to predictions of two-stage melting in 2-d, with a distinctive "hexatic" intermediate phase [11.2].

For a 2-d lattice it is well known that long-range order can exist in a situation with only short-range interactions: witness the celebrated ONSAGER solution to the Ising model [11.3]. Other less familiar models have also recently been solved in 2-d (e.g., hard hexagon or three-state Potts class [11.4a], triple spin or Baxter-Wu or four-state Potts [11.4b], and eight vertex [11.4c]), while none have been solved exactly in 3-d (save the spherical model [11.5a]; the infinite-d spin "Ising" model has a nearly identical solution [11.5b,c]). A number of theoretical techniques, described in Sect.10.2.3 (this chapter introduces many of the lattice gas concepts relied on here), have been developed to deal generally with the features of a 2-d lattice. A particularly favorable trait of 2-d second-order transitions

is that the critical region is orders of magnitude larger than in 3-d, making experimental observation considerably easier.

To test the theories associated with 2-d critical phenomena, one needs genuinely 2-d systems, rarities in nature. Atoms adsorbed on essentially passive surfaces offer the desired 2-d properties. Several recent conferences have explored this exciting area [11.6,7]. Fortunately, their proceedings, in most cases, have been published [11.6], making this progress available to a wide audience. Two excellent reviews [11.8,9] will appear soon, too. The current presentation will only be able to focus on a limited selection of topics. The hope is to whet the reader's appetite by presenting some highlights of special interest to those studying adsorption. We assume some familiarity with surface science but very little with progress in static critical phenomena. (An outstanding series of review articles is in [11.10].)

In Sect.11.2, a general introduction to critical properties is given. The ideas of critical exponents, corrections to scaling, and crossover phenomena are presented in terms appropriate to surface science. Section 11.3 discusses order parameters and universality classes. "Universal" features do not depend on any of the explicit parameters of a system, just on symmetries and dimensionality. This section presents a general scheme for determining what sorts of universality classes can be found in commensurate adsorption systems. Section 11.4 discusses how LEED measurements can probe critical phenomena and explores some of the problems that arise in actual experiments, notably substrate disorder. Section 11.5 describes the few experiments undertaken to measure critical exponents for adsorbed overlayers. The only chemisorption case so studied, O/Ni{111}, is examined carefully. Section 11.6 mentions some implications of this work.

11.2 Important Concepts

11.2.1 Lattice Gas Model

An important feature of all chemisorption and most physisorption systems is that, at low coverages, the adatoms sit at specific positions relative to the substrate atoms. Thus, it is appropriate to describe these systems with lattice gas Hamiltonians [see (10.1)]. For present purposes, all but the first few pairwise interactions E_i can be neglected. We remind the reader that these E_i fall off rapidly in magnitude with increasing separation and, in the case of chemisorption on transition metals, are anisotropic and can

be attractive or repulsive. These pairwise interactions, as well as higher order interactions, were reviewed in ISISS 1977 [11.11]; there has since been progress in calculating signs and rough magnitudes for H on narrow-band transition metals [11.12], as well as in general understanding [11.13]. We emphasize the distinction from physisorption, where the E_i's originate essentially from van der Waals forces and so are invariably strongly repulsive at small spacings R_i, then (decreasingly) attractive for larger R_i.

In chemisorption, as opposed to physisorption, the binding energy is so much larger than the E_i's that the fractional coverage $\theta = \mathcal{N}/N$ [N being the number of lattice sites, $\mathcal{N} = \sum n_i$ the number of adatoms] is essentially fixed at temperatures of order to E_i/k_B, at which 2-d phase transitions occur (in contrast to physisorption). The phase transitions that concern us here are order-disorder processes. These are the only kind that occur in simple systems with only a few repulsive pair interactions and no attractions. The intuitive picture is that adatoms try to avoid each other but are "forced" closer together by increased coverage. For example, in the case of a square lattice with only nearest neighbor repulsions, the adatoms occupy sites randomly at low θ, but (at low temperatures) for some θ between 1/4 and 1/2 form an ordered checkboard pattern with only one "color" of site occupied (to avoid the penalty energy E_1). As temperature increases, the entropy gained by occupying both sites outweighs the energy considerations in the free energy, and the $c(2\times 2)$ pattern disorders (cf. R = 0 curve [11.14] in Fig.10.1). The important feature in determining critical behavior is the number and symmetry of equivalent sites available for disordering. A second kind of transition occurs at low coverages when attractive interactions are present. Then, ordered islands form, e.g., in the square lattice gas case, an attractive E_2 leads to ordered checkboard islands at coverages well below 1/4 (in fact down to 0). With increasing temperature, adatoms "evaporate" into the gas background, with associated latent heat; the transition is first order. At higher coverages, one again encounters order-disorder type transition (cf. R = -1, -1/2 plots [11.14] in Fig.10.1).

We recall the expression for expectation values of observables given in (10.2). At high temperatures, all sites are occupied with equal probability, formally $\langle n_i \rangle = \theta$ and more importantly $\langle n_i\, n_j \rangle = \theta^2$, for all i,j. Below the transition temperature T_c, the lattice sites can be imagined as dividing into a [small] number of sets of equivalent sites having some lower symmetry than the lattice as a whole. Each set has the same number of sites.

As we shall see more clearly below, the idea is that below T_c one of these sets is preferentially occupied.

11.2.2 Critical Exponents and Scaling Laws

The measurable thermodynamic properties are usually defined in terms of the analogous magnetic Hamiltonian for spins on a lattice. Thus the independent variables are magnetic field h and temperature T [or often more conveniently, reduced temperature $t \equiv (T - T_c)/T_c$]. In chemisorption experiments one measures the divergences of the correlation length $\xi\{\langle s_i\, s_j\rangle \sim \ln(R_{ij}) \times \exp(-R_{ij}/\xi)\}$ in 2-d and the susceptibility $\chi[|-(\partial^2 F/\partial h^2)|_T]$ with decreasing $|t|$,

$$\xi \propto |t|^{-\nu} \quad ; \quad \chi \propto |t|^{-\gamma} \quad . \tag{11.1a}$$

The "magnetization", i.e., the order parameter (to be defined shortly) vanishes as

$$m \propto (-t)^{\beta} \quad [t < 0 \ \text{only}] \quad . \tag{11.1b}$$

Expressions for these measurables in magnetic language are given in most general reviews [11.15,16]; we shall encounter their adsorption appearance in Sect.11.4. In addition, we mention the specific heat

$$C = (kT^2)^{-1}(\langle \mathcal{H}^2\rangle - \langle \mathcal{H}\rangle^2) \propto |t|^{-\alpha} + \text{const.} \tag{11.1c}$$

While this quantity cannot be measured in chemisorption, it can sometimes in physisorption and is useful in Monte Carlo simulation. Other exponents are not readily accessible.

This Greek alphabet soup is dramatically simplified by the *scaling hypothesis*. This experimentally corroborated idea states that the divergence of ξ (i.e., the long-range correlations of fluctuations near T_c) is responsible for all singular behavior; ξ is the only relevant length in determining the singular behavior at criticality [11.16]. This hypothesis is consistent with the independence of critical exponents from details of the microscopic Hamiltonian and the lattice constant. One consequence of the hypothesis was used implicitly in writing (11.1a,c), namely, that α, γ, and ν are the same above and below T_c (note that the proportionality constants are *not* identical). More generally, only two exponents are independent; this statement is expressed in "[hyper]scaling laws,"

$$\alpha = 2(1 - \nu) - \nu(d - 2) \quad , \tag{11.2a}$$

$$\gamma = 2(\nu - \beta) + \nu(d - 2) \quad . \tag{11.2b}$$

The laws are written so as to emphasize their particularly simple form for d = 2.

11.2.3 Corrections to Scaling

When confronting experimental curves, (11.1) indicates that fits of observables G(T) require the nonlinear form,

$$G(T) = A_{\pm}|T - T_c|^{\lambda} \quad . \tag{11.3}$$

Note that in general T_c must be determined simultaneously with the exponent λ and the [nonuniversal] amplitude A. To do the fit, we usually want $G(T_c) = 0$, not ∞; for divergent quantities we need merely fit the inverse. Further complications do exist, however. The simple form of (11.1,3) is just the first term of a power series, $t^{\lambda}[1 + Dt + \ldots]$. Often there are other weaker ["confluent"] singularities at T_c leading to corrections of the form

$$|t|^{\lambda}[1 + D_{1,\pm}|t|^{\Delta 1} + D_{2,\pm}|t|^{\Delta 2} + \ldots] \quad , \tag{11.4}$$

where Δ_1 and Δ_2 are not integers [11.17]. Since all the D's are nonuniversal and the Δ's are model dependent, general statements are difficult, if not impossible. For the particular case of the 2-d Ising model, for which a detailed solution is available (but for which corrections of the form (11.4) do not occur [11.18]), ROELOFS [11.19] investigated the dependence of the effective value of ν on the range of t analyzed. For $t_{min} = 0.005$ and 0.02, he found the deviation (underestimation) to be less than 5% for $t_{max} \leq 0.09$ and 0.06, respectively (cf. Fig.11.1). There is some evidence

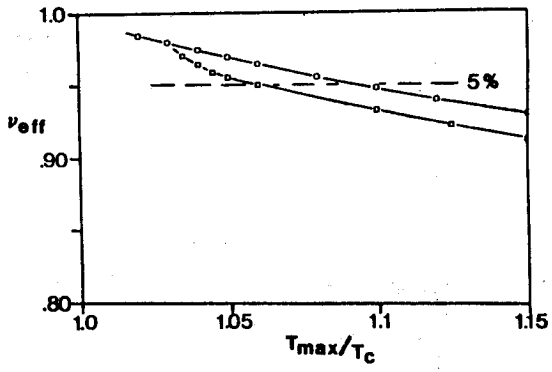

Fig.11.1. Variation of the effective value of ν vs the upper limit of the fitting range, T_{max}, for the Ising model solution for inverse correlation length [11.20]. The circles are for T_{min}=1.005 and the squares for T_{min}=1.02 [11.19]

[11.18] that such effective exponents, deduced for some common range, obey the scaling laws of (11.2), although it is not presently certain how generally this is true. Under certain circumstances, associated with a parameter being "marginal" (not changing under scale increases at the "fixed point" representing the transition), the correction is logarithmic [11.21],

$$|t|^{\lambda}(1 - u_{\pm}\ln|t|)^{\tau} \quad . \tag{11.5}$$

In this case the correction term becomes worse [larger] as t_{min} decreases. The size of the correction is partially determined by the nonuniversal [i.e., dependent on specifics of the system] coefficient u. We shall encounter such a case below, the four-state Potts model [11.21][1]. Since conclusive experimental demonstration of logarithmic corrections requires decades of t range, it is particularly favorable to investigate lower dimensionalities, where critical regions are relatively large.

11.2.4 Crossover Phenomena [11.22]

Often real systems do not correspond perfectly to simple models but contain small admixtures of other models having different-symmetry ground states. Some examples for magnetic systems are weakly anisotropic systems or layered systems with primarily 2-d coupling and weak 3-d coupling between layers. We shall encounter, in Sect.11.3.4, 5 the case of {111} fcc [or {0001} hcp] surfaces, when a honeycomb lattice of threefold sites is split by a weak crystal field into two triangular lattices. Such systems have the form

$$H = H_0 + gH_1 \tag{11.6}$$

where $\langle H_1 \rangle_{g=0} = 0$.

Far from T_c, the system appears to be in the universality class associated with H_0, as though g were zero. Very close to T_c, the system senses the symmetry of the full H and responds according to its [different] universality class. Note that this new behavior implies not only a different set of critical exponents but also a different, g-dependent critical temperature. At intermediate temperatures the system crosses over from one class to the other. By the scaling hypothesis, the intermediate behavior can be written as, e.g., for susceptibility,

1 If u vanishes, so does the logarithmic correction. Such may be the case for the Baxter-Wu model [11.4b], which is in the same universality class as the four-state Potts model but exhibits pure power law behavior [11.21].

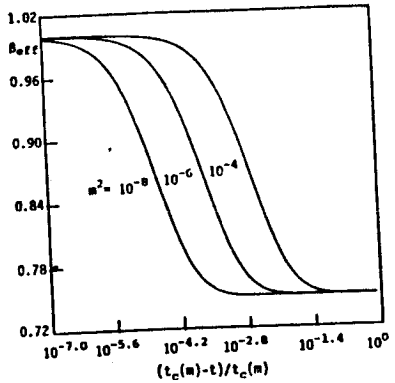

Fig.11.2. Illustration of effective exponents in a crossover regime for what amounts to three different values of g [11.23]

$$\chi(T,g) \propto t^{-\gamma}X(g/t^{\phi}) \tag{11.7}$$

where t is reduced with respect to $T_c(g = 0)$ and the crossover scaling function X(z) is normalized by X(0) = 1. The crossover scaling exponent ϕ has the form $\phi = \zeta\nu$, where ζ is an exponent associated with scaling the field of H_1 and ν is familiar by now. The crossover region thus occurs for $t \sim g^{1/\phi}$; its width is determined by the explicit, system-dependent form of X(z).

In a graph of ln(G) vs ln|t|, the curve is nearly linear for large and small |t|, and bends smoothly between these limits. The effective exponent, defined by $\partial \ln(G)/\partial \ln|t|$, has the value associated with H_0 for large |t| and with H for small |t|. In between, it varies continuously from one to the other, and cannot be neatly defined as some weighted average. Figure 11.2 illustrates this idea [11.23]. Note that *if* we knew we were in a well-defined critical region, a way to fine-tune a fit would be to minimize the curvature of ln(G) vs ln|t| with respect to T_c.

The crossover also applies near tricritical points, described in Sect. 10.3.3. Tricritical points have their own set of exponents, often with smaller β than that of the adjoining second-order line [11.24]. In this vicinity one could see (depending on some details) the tricritical exponents until one gets close to that line, then crossover to those of the line (or to a weak first-order transition). To illustrate the complexities inherent to this region, we cite a very recent impressive study of the disordering of $(\sqrt{3} \times \sqrt{3})$ Kr physisorbed on (ZYX exfoliated) graphite [11.25]. With X-rays from a synchrotron, resolution (HWHM = 3.5×10^{-4} Å^{-1}) two orders of magnitude better than LEED studies of Sect.11.5 were obtained. The measured value of β, 0.065 ± 0.015, was somewhat larger than the predicted β_M of the

tricritical point but much less than the predicted second-order line β [which is (nearly) double β_M].

11.2.5 Fisher Renormalization

Another more general caveat concerns Fisher renormalization [11.26]. Although ideal exponents are calculated with the external field (i.e., the chemical potential for a lattice gas) as the independent variable, for chemisorption it is the conjugate variable, the coverage, that one can control. When a quantity, in this case θ, that would vary critically at a second-order transition is constrained, the measured exponents will change. Figure 11.3 illustrates schematically the essence of this situation, showing lines of constant μ in a second-order phase boundary in a θ-T plot. The singular variation of these lines at the critical point has the effect of exponentially renormalizing the reduced temperature by $1/(1 - \alpha)$ to lowest order. Accordingly, divergences in $|t|$ are renormalized; $\lambda \to \lambda/(1 - \alpha)$, where $\lambda = \beta, \gamma,$ and ν, but $\alpha \to -\alpha/(1 - \alpha)$. Note that the scaling laws (11.2) still hold for these renormalized exponents. Note also that, since $\alpha = 0$ for the Ising model, fixing θ does not renormalize exponents (although there are subtle logarithmic effects). Inspection of Fig.11.3 suggests that one expects to measure the ideal, unrenormalized exponents until one gets close to the boundary, where there is crossover to the renormalized values. The crossover region happens at smaller and smaller reduced temperatures as one approaches the symmetry line interacting with the apex of the boundary. To date, no conclusive experimental observation of Fisher renormalization has been reported; with their large critical regions and intrinsically constrained θ, chemisorption systems present a propitious hunting ground.

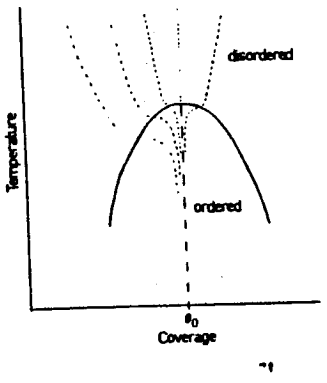

Fig.11.3. Illustration of the source of Fisher renormalization. The solid line denotes second-order transitions. The (dashed) lines of constant chemical potential vary singularly at the transition, except at the maximum, $T_c(\theta_0)$. Constraining θ rescales temperature near $T_c(\theta)$ over a range which vanishes near $T_c(\theta_0)$ [11.19]

The implications of Sect.11.2.4,5 for experimentalists are twofold. When it is feasible, measure critical exponents away from a crossover regime before tackling that complicated domain. When near such a regime, plot ln(G) vs $\ln|t|$ to see if well-defined critical behavior is monitored.

11.3 Universality Classes for Atoms on a 2-d Lattice

11.3.1 Order Parameters

The details of phase transitions are best discussed in terms of an order parameter ψ which can be a scalar, a vector, or a tensor of higher rank. By definition it vanishes above T_c, when there is no long-range order, and it is usually normalized to unit magnitude for a fully ordered state. In a second-order transition, $|\psi|$ moves continuously from 0 as T drops below T_c, while in a first-order one, it jumps discontinuously.

Some simple examples are helpful. For the checkerboard $c(2\times2)$ pattern discussed earlier $\psi = (N_A - N_B)/(N_A + N_B)$ where A and B denote the two "colors" of sites and N_I the total occupation of each (10.7). For the $(\sqrt{3} \times \sqrt{3})R30^\circ$ pattern on a triangular lattice (commonly observed in physisorption, as alluded to in Sect.11.2.4), in which there are three equivalent sites, we might write

$$\underline{\psi} = \frac{N_A\hat{x} + N_B\left(\frac{-\hat{x} + \sqrt{3}\hat{y}}{2}\right) + N_C\left(\frac{-\hat{x} - \sqrt{3}\hat{y}}{2}\right)}{N_A + N_B + N_C} \quad . \tag{11.8}$$

This vector is often more conveniently discussed in terms of two orthogonal components.

11.3.2 Universality Classes

Writing the free energy of the system as $F(T,\psi)$, we note that the minimum of F lies at $\psi = 0$ for $T > T_c$. In a second-order transition, this minimum moves infinitesimally away from $\psi = 0$ as T drops infinitesimally below T_c. If we expand $F(T \lesssim T_c, \psi)$ about $F(T \lesssim T_c, 0)$, we expect the lowest order term, in ψ^2, to be negative and the higher order terms positive. The explicit form of the expansion of F in powers of ψ thus determines the behavior of the system near T_c, i.e., it determines the critical properties. Each distinct expansion corresponds to a different universality class. The expansion obtained for a lattice gas system can also be obtained from some spin-spin interaction system which often bears no initially obvious relation-

ship to the ordered overlayer pattern; but the analogy does give deeper understanding of how the overlayer disorders. The name of the magnetic system conventionally denotes the universality class.

The simplest magnetic interaction is of the form

$$\mathcal{H} = -J \sum_{<jk>} \underline{s}_j \cdot \underline{s}_k = -J \sum_{<jk>} \sum_{i=1}^{n} s_j^{(i)} s_k^{(i)} \tag{11.9}$$

for n-d spins. For n = 1, 2, and 3, these systems are called Ising, XY (or planar rotor), and Heisenberg, respectively. From symmetry considerations alone one can write the expansion as

$$F(T,\psi) = F(T,0) + r \sum_{i=1}^{n} \psi_i^2 + u_2\left(\sum_{i=1}^{n} \psi_i^2\right)^2 + u_3\left(\sum_{i=1}^{n} \psi_i^2\right)^3 + \ldots \tag{11.10}$$

where ψ_i is $\sum_j s_j^{(i)}$, and r is proportional to $T - T_c$ and so changes sign at T_c. For spins without full n-d rotational symmetry, there are further terms in the expansion. The general procedure for constructing these expansions using group theory is well developed but rather technical (the classic, detailed, semiscrutable exposition is [11.28]; also [11.29]). Landau gave three rules, couched in [group] representation language, for determining whether a particular expansion in order parameter can produce a second-order transition. Since this approach is in essence mean-field-like, one must check whether fluctuations destroy the claims. Indeed, for d = 2, the second Landau rule is violated (by the three- and four-state Potts models). We emphasize that these symmetry-based considerations indicate only whether a particular overlayer can have a continuous transition; whether it actually will depends on the expansion parameters in the expansion of F, and so, ultimately, on the lattice gas interactions E_i.

Most of the applications of these ideas to adsorption systems have been carried out by DOMANY, SCHICK, and co-workers [11.30]. SCHICK's excellent recent review [11.9] is uniquely readable from a surface science perspective. Most of the remainder of Sect.11.3 presents highlights and results of that treatment.

11.3.3 Landau Theory for Adlayers

The ordered state below T_c can be described by some 2-d wave vector $\underline{Q}$. However, if we include some Q, we must also admit all [say ℓ] independent members of its "star," i.e., all other wavevectors generated by applying the point-group operations of the lattice of adsorption sites (hereafter the

"net"), that are not related by a reciprocal lattice vector g of the net,

$$\langle n_i \rangle = \theta + \sum_{s=1}^{\ell} \rho(\underline{Q}_s) \exp(i\underline{Q}_s \cdot \underline{R}_i) \quad . \tag{11.11}$$

If some $\underline{g}$ connects $\underline{Q}_s$ and $-\underline{Q}_s$, then $\rho(\underline{Q}_s)$ is real and

$$\langle n_i \rangle = \theta + \sum_{s=1}^{\ell} \rho(\underline{Q}_s) \cos(\underline{Q}_s \cdot \underline{R}_i) \quad , \tag{11.12}$$

otherwise $\rho(\underline{Q}_s) = C(\underline{Q}_s) + i\, S(\underline{Q}_s)$ with C and S real, and

$$\langle n_i \rangle = \theta + 2 \sum_{s=1}^{\ell/2} C(\underline{Q}_s) \cos(\underline{Q}_s \cdot \underline{R}_i) + 2 \sum_{s=1}^{\ell/2} S(\underline{Q}_s) \sin(\underline{Q}_s \cdot \underline{R}_i) \quad . \tag{11.13}$$

The first Landau rule states in essence that for a second- order transition there is just a *single* [star of] $\underline{Q}$ needed to describe the ordered state.

Now in the first case, the ρ's are the ensemble averages of the ℓ-component order parameter,

$$\psi_s = N^{-1} \sum_i n_i \cos(\underline{Q}_s \cdot \underline{R}_i) \quad s = 1,\ldots,\ell \quad , \tag{11.14}$$

while in the latter case it is

$$\psi_s = N^{-1} \sum_i n_i \begin{cases} \cos(\underline{Q}_s \cdot \underline{R}_i) & s = 1,\ldots, \ell/2 \\ \sin(\underline{Q}_s \cdot \underline{R}_i) & s = 1,\ldots, \ell/2 \quad (2^{\text{nd}}\ \ell/2 \text{ components}). \end{cases} \tag{11.15}$$

To illustrate the formalism, note that for the checkerboard $\underline{R}_i = (m,n)$ and $\underline{Q}_s = \pi(1,1)$, so we recover the single component $\psi = N^{-1} \sum n_i (-1)^{m+n}$. For th $\sqrt{3}$ pattern we have $\underline{R}_i = [(1/2)(m + n),\ (\sqrt{3}/2)(m - n)]$ and take $\underline{Q} = (4\pi/3)(1,0)$. Then $N^{-1} \sum n_i \cos[(2\pi/3)(m + n)]$ and $N^{-1} \sum_i n_i \sin[(2\pi/3)(m + n)]$ give the x and y components, respectively, of $\underline{\psi}$ as set down in (11

The third Landau rule, also called the Lifshitz criterion, requires that $\underline{Q}$ be at a high symmetry point of the surface Brillouin zone (SBZ): either t origin or a symmetry point on the edge. This condition selects which commer surate overlayers can undergo continuous transitions; they must be relative dense [11.31]. The actual criterion is somewhat more stringent. Continuous transitions are still possible to incommensurate states, which are not dis cussed here [11.28-30].

Landau theory also shows how to generate the free-energy expansion sole on the basis of symmetry. The m^{th}-order term in the expansion contains pro ducts,

$$\rho(\underline{Q}_a)\rho(\underline{Q}_b) \cdots \rho(\underline{Q}_m) \quad . \tag{11.16}$$

In order for translation invariance to be satisfied, the sum of these m $\underline{Q}$'s must be a $\underline{g}$. Furthermore, the free energy (and hence each order in the expansion) must be invariant under the point group operations of the net. Since some of these operations interchange some of the Q's, the products must be symmetric under this interchange, or there must be other m^{th}-order products. Observe that this approach gives no information about the coefficients of the terms in the expansion.

11.3.4 Catalogue of Transitions

Table 11.1 summarizes the assignment of adatom overlayer transitions to universality classes. It is quite remarkable how few universality classes there are and also how few of the experimentally observed overlayer patterns [11.32] are able to undergo second-order transitions.

Table 11.1. Overlayer patterns, on nets with common symmetries, which can have continuous order-disorder transitions. Adapted from [11.9]

Universality class and exponents / Substrate symmetry	Ising	x-y with cubic anisotropy	3-state Potts	4-state Potts
	α 0(log) β 1/8 γ 7/4 ν 1	non universal	1/3 1/9 13/9 5/6	2/3 1/12 7/6 2/3
Skew (p1) or rectangular (p2 mm)	(2 × 1) (1 × 2) c(2 × 2)			
Centered rectangular (c2 mm) or square (p4 mm)	c(2 × 2)	(2 × 2) (1 × 2) (2 × 1)		
Triangular (p6 mm)			$(\sqrt{3} \times \sqrt{3})$	(2 × 2)
Honeycomb (p6 mm)	(1 × 1) [p(2 × 2)][a]			(2 × 2)
Honeycomb in a crystal field (p3 m1)			$(\sqrt{3} \times \sqrt{3})$	(2 × 2)

[a] Heisenberg with corner cubic anisotropy ($K_4 \lesssim 0$)

The most common class in the table is Ising. This class results whenever the order parameter has a single component; there is no possibility of extra terms in (11.10). In the rectangular case [e.g., {110} fcc], the three overlayer patterns correspond to $\underline{Q}$'s pointing to the center of either of the sides of the rectangular SBZ or to a corner. Since $\underline{g}$'s connect any one to any other member of its star, each star contains just one independent member. Similar remarks apply to the square lattice [e.g., {100} bcc, fcc] when $\underline{Q}$ points to a corner of the SBZ or to the centered rectangle [e.g., {110} bcc] when it points to the middle of the short edge. The c(2 × 2) overlayers are unusual in that the lattice gas Hamiltonians can actually be transformed into the Ising model by a familiar change of variables [that is, substitute $(s_i + 1)/2$ for n; (see Sect.10.3.1)]; thus, the correspondence holds not just near T_c but for all T. For the honeycomb, the situation is a bit more complicated since the lattice is not Bravais. The (1 × 1) pattern corresponding to $\underline{Q} = 0$ has one of the two triangular sublattices occupied. SCHICK's careful treatment [11.9] contains numerous figures to illustrate these comments. Discussion of the p(2 × 2) overlayer, corresponding to a Heisenberg model with cubic anisotropy, is deferred to Sect.11.5.

In the square lattice case (that of the centered rectangle is quite similar), if $\underline{Q}$ points to the middle of an edge, we find

$$\begin{aligned} n_i &= \theta + (\underline{Q}_i)\cos(\underline{Q}_1 \cdot \underline{R}_i) + \rho(\underline{Q}_2)\cos(\underline{Q}_2 \cdot \underline{R}_i) \\ &= \theta + (-1)^m\rho(\underline{Q}_1) + (-1)^n\rho(\underline{Q}_2) \end{aligned} \tag{11.17}$$

if we write $\underline{R}_i = (m,n)$. This form describes a (2 × 2). If either $\rho(Q_1)$ or $\rho(Q_2)$ happens to vanish, we have a (2 × 1). Since $\ell = 2$, we start with (11.10) with n = 2, an XY model. There is an additional fourth-order term of the form $w[\psi_1^4 + \psi_2^4]$, or equivalently $w'\psi_1^2\psi_2^2$, arising because the point group of a square is lower than full rotational. In magnetic language, a term $S_x^4 + S_y^4$ is added to (11.9), favoring either the two coordinate axes or the diagonals depending on the sign of the coefficient. It is somewhat perversely referred to as "cubic anisotropy" since a square is a 2-d cube. This model is highly unusual in that its exponents are nonuniversal [11.33], depending on the particulars like interaction strengths and coverage. As this situation has no parallel in 3-d, it offers an unusual opportunity for surface science to advance insight into critical phenomena [11.9]. On the other hand, it seems bold if not foolhardy to investigate such a system before one has mastered the study of systems with firmly known exponents.

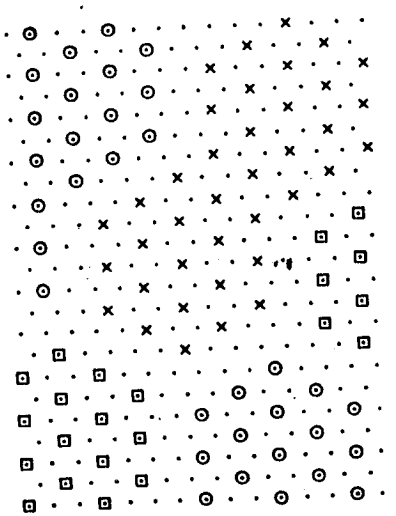

Fig.11.4. Several clusters of ordered $(\sqrt{3} \times \sqrt{3})R30^\circ$ regions, to motivate the correspondence to the three-state Potts model near T_c

Triangular lattices [e.g., atop binding on {111} fcc or {0001} hcp, centered sites on basal graphite] have as their SBZ a regular hexagon. As alluded to in Sect.11.3.3, a $(\sqrt{3} \times \sqrt{3})R30^\circ$ is produced by a $\underline{Q}$ pointing to a vertex of the hexagon. Since its negative is not connected by a $\underline{g}$, the slightly more cumbersome form of (11.15) was needed. The order parameter was seen to have two components. In addition to the terms of (11.10), there is a third-order term $\psi_1^3 - 3\psi_1\psi_2^2$ (violating the second Landau rule). This expansion is the same as that of the three-state Potts model [11.34], where the n-state Potts model [11.35] is defined by

$$\mathcal{H} = -J \sum_{<i,j>} \delta_{s_i,s_j} \qquad (11.18)$$

with s_i having n possible values (or directions or "colors"). Note that the two-state Potts model is just the Ising model. An intuitive grasp of the origin of this correspondence can be gained by examining Fig.11.4. Near T_c it is not the interaction of individual adatoms but rather those of large ordered clusters which determine the physics. In the $\sqrt{3}$ pattern there are three subsets of sites. There is one kind of domain wall (and resulting interaction energy) between clusters occupying the same subset. The walls between clusters on differing subsets do not depend on which two subsets are involved, but do depend on orientation. The figure shows the [two kinds of] antiphase boundaries that occur for strongly repulsive E_1. For weaker E_1, the domains approach each other closer. Computation of an effective cluster-cluster

Hamiltonian of the form (11.18) requires averaging over the many possible borders, often with some ab initio insight; such practice is implicit in the prefacing transformations [11.6b,8,36] mentioned in Chap.10.

A second star contains vectors pointing to the middle of the edges of the SBZ and generates (2×2) overlayers. Opposite $\underline{Q}$'s are related by $\underline{g}$'s. One finds that n = 3; the extra terms to be added to (11.10) are $w\psi_1\psi_2\psi_3$ and $v \sum_{i=1}^{3} \psi_i^4$, producing the expansion of the four-state Potts model. The logarithmic corrections associated with this model (see footnote 1) relate to the fact that, as a function of the (not necessarily integral) "number" of states, 4 is the largest at which a second-order transition occurs [11.37

A honeycomb lattice is provided by the center (three-fold) sites of a close-packed layer of atoms. In physisorption this can be achieved by preplating based graphite, typically with Kr. The {111} faces of face-centered cubic crystals and {0001} faces of hcp crystals would also have this symmetry were it not for the second layer. The crystal field provides a binding-energy difference between those sites directly over atoms in the second layer (hcp sites) and the other half of the sites (fcc sites). This "staggered field" is expected to be small from solid-state experience.[2] From Sect.11.2.4 we recall that "well away" from T_c we can neglect this splitting.

While the honeycomb lattice has a triangular Bravais net, the two-site basis complicates the analysis. It turns out [11.30c] that the two-element star with Q's pointing to opposite vertices no longer satisfies the group theoretic expression of the Lifshitz condition.

There is, however, a new rich situation having the three-component star. The free energy has the extra term $w \sum_{i=1}^{n} \psi_i^4$. The ψ_i's are not just the $\rho(\underline{Q})$'s, but correspond to a 3-d (spin) vector. The extra term provides cubic (truly, this time!) anisotropy. For w positive, the six faces of the spin cube are favored. The adatoms form a (2×1) structure, occupying alternate rows in one of the three principal directions (for a total of six possible states). The transition has been recently shown to always be first order [11.39]. For w negative, eight concerns of the spin cube are favored. This case is discussed at the end of Sect.11.5.

---

2 We expect E_0 to be comparable to the stacking fault energy per atom for the substrate. This energy is well known to be small, on the order of ter of meV, and can vary by about an order of magnitude among metals [11.38].

11.3.5 Percolation

When all the E_i's of an overlayer are repulsive, the onset of long-range order occurs at roughly the same coverage for a wide range of temperatures (cf. R = 0 curve [11.14] in Fig.10.1). BINDER and LANDAU [11.14b] noticed that this coverage can be related to a (site-)percolation threshold: We imagine small planar objects with size determined by the area excluded on the lattice by repulsive E_i's. These objects are placed at random (but without overlap) on lattice sites. A cluster is defined as a set of these touching one another. As more of these objects are deposited, the size of the largest cluster starts to grow rapidly and suddenly girds the lattice (via periodic boundary conditions). In an infinite system, we say that the mean size of finite clusters diverges at a critical coverage θ_c, the percolation threshold.

Percolation has received much attention over recent years (a comprehensive review is in [11.40], also [11.41]). In spite of the absence of a Hamiltonian or a partition function [11.41c], it has been possible to draw analogies between functions describing the percolation problem and those describing a ferromagnet. Specifically, the mean size of finite clusters corresponds to the (zero-field) susceptibility, the mean number of clusters to the free energy, the fraction of sites in an infinitely large cluster ("percolation probability") to the magnetization, and the pair connectedness to the pair correlation function. The analogue of t is $\theta_c - \theta$. Following (11.1), we can define critical exponents. The percolation problem has been shown to correspond to the one-state Potts model [11.41], which has conjectured exponents [11.24b] $\nu = 4/3$, $\beta = 5/36$; thus, with the scaling equation (11.2), $\alpha = -2/3$, and $\gamma = 43/18$. It is not yet clear how fruitful such insights will prove to be for chemisorbed atoms .

11.4 LEED on Single Crystal Faces

11.4.1 Measurement of Exponents

In the remainder of this review, we shall specialize on the investigation of chemisorbed atoms on faces of metallic single crystals using LEED. Since it interacts strongly with matter, LEED is a natural probe of surface phenomena. There is no need for the enormous "surface" of exfoliated graphite required for neutron or (to date) X-ray scattering. Its resolution is at present as good as neutrons [11.42], and some new apparatuses are or will soon be capable of about a two-orders-of-magnitude improvement [11.43]. The technique is convenient. Most surface science laboratories have the needed equipment; there is no need to suffer the travails involved in experiments at a large multiuser facility. For over a decade, LEED has been used primarily for probing interatomc distances. This procedure involves an arduous effort due to the potent effect of multiple scattering [11.44]. In studying critical exponents, we use LEED for what it does best and most naturally: monitoring order on the surface. Many of the distinctions between chemisorption and physisorption were discussed in Sect.11.2.1. Because of the far greater binding energies, it is much easier to do LEED, making the delicate procedures developed by FAIN (Chap.9) unneccessary. Moreover, the greater strength of interactions leads to T_c's higher by half an order of magnitude; the size of the critical region, which is linked to reduced temperature, is scaled up accordingly in absolute temperature.

In LEED, in the kinematic limit, the intensity measured is the Fourier transform of the two-site correlation function,

$$I(k) = \mathscr{F}\{\langle n_i n_j \rangle\}$$
$$= \mathscr{F}\{\langle [n_i - \langle n_i \rangle][n_j - \langle n_j \rangle] \rangle + \langle n_i \rangle \langle n_j \rangle\} \qquad (11.19)$$

where the second term in braces is the product of the mean occupation of two sites and the first is the correlation of fluctuations (about these means) for the sites. Recalling (11.11), we note that for ordered overlayers we are interested in $n_j \exp(i\underline{Q} \cdot \underline{R}_j)$ rather than just n_j. Second, we must account for the fact that adatoms bind only to a particular lattice of sites with an associated reciprocal lattice. Third, the Fourier transform of the 2-d correlation function is Lorentzian. Thus, the intensity *due to the overlayer* is [11.20,45]

$$I(\underline{k}) \propto \sum_{\underline{Q}_s, \underline{g}} \left[\frac{\chi(\underline{Q}_s + \underline{g}, T)}{(\underline{Q}_s + \underline{g} - \underline{k})^2 + \xi^{-2}} + A\delta_{\underline{k}, \underline{Q}_s + \underline{g}} |t|^{2\beta} \theta(-t) \right] \qquad (11.20)$$

Thus, the LEED beams of interest are those at $\underline{Q}$ and its star, and all others related to them by reciprocal lattice vectors. In non- Bravais cases, the situation may be more complicated, e.g., glide planes can eliminate beams (Chap.9). We reemphasize that the $\underline{g}$'s are those due to the adsorption sites, not the atoms of the top layer of the substrate. For bridge sites on a square lattice, the lattices differ by $\sqrt{2}$ in lattice constant and 45° in orientation For bridge sites on a triangular lattice or centered sites on a honeycomb net, even the symmetries are different (Kagomé and triangular, respectively).

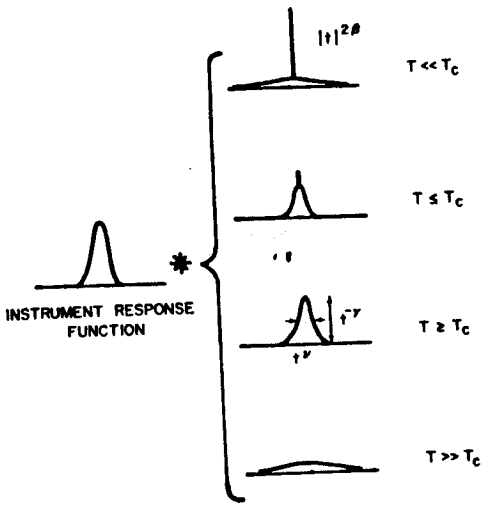

Fig.11.5. Schematic of adlayer-induced LEED spots vs k at various temperatures

The astute LEED practitioner may recognize that these beams of interest are just those that PARK long ago noted would be broadened by interference between antiphase domains [11.46]. The vectors connecting sites across the antiphase boundary are seen to be primitive vectors of the lattice of adsorption sites. Thus, in many cases, observation merely of which beams are broadened by critical scattering can identify the binding site and hence, in conjunction with the adlayer-induced spot pattern, predict the universality class of the transition.

Recalling (11.1) we see that the amplitude of the critical scattering goes as $t^{-\gamma}$ while its width goes as t^{ν}, as illustrated in Fig.11.5. As also shown, analysis of this behavior is confounded by the LEED instrument response function, which is convoluted with the ideal scattering of (11.20) in any measured profile. This function can be obtained from a low-temperature beam profile, where critical scattering is insignificant. Our procedure for removing the instrumental effects will be discussed in the next section, in conjunction with our case study [11.19,47]. (A preliminary account with some inaccuracies in the exponent analysis is in [11.6b].)

Heretofore many researchers, particularly those using weakly interacting probes (X-rays or neutrons), suspected that the strong interactions of electrons would preclude their use in studying critical exponents. The fear was that in addition to $\langle n_i n_j \rangle$ one would unavoidably collect multisite correlations like $\langle n_i n_j n_k \rangle$. Fortunately, the atomic scattering factor for light atoms below 50 eV is peaked in the backward and (more strongly) in the forward directions, with very little probability for right-angle scattering

[11.48]. If the incident beam is oriented normal to the surface, an electron is likely after (or before) scattering off an adatom to strike substrate atoms below the adatom. This sort of process leads to the multiple scattering that makes LEED I-V analysis so complicated. A process involving scattering off one adatom, then a second with subsequent escape requires a right-angle scattering followed by (for low-order spots) another nearly right-angle scattering. Such processes, which introduce the feared multiadatom correlations, are highly improbable and hence of very small amplitude. The effects of the preceding sort of process do not vary significantly near T_c since the substrate does not participate in the transition; accordingly, any modulation of the beam profile can be removed more or less in the pursuit of the known general form of the critical behavior.

11.4.2 Surface Defects

Finally, we discuss the nonideal nature of metallic crystal surfaces used in chemisorption. This problem involves not just the finite size of plateaus but also defects thereon. This sort of difficulty may well be intrinsically more stubborn here than in physisorption because the same chemical aspects of a surface promoting strong adsorption bonds renders it vulnerable to defects or distortions; the strong interplane bonding of planar materials like graphite make them poor chemisorbers [11.49].

The effect of the finite extent of perfectly flat areas on the surface is to raise T_c and to round (blur) the transition. Both effects are proportional to $L^{-1/\nu}$, where L is the linear dimension of a flat region; this dependence is useful for Monte Carlo but not of much use to the experimentalist unless the surface can be systematically damaged. The typical size of L is 100-200 Å in good samples; once ξ approaches this size, the effects become important. Note that probing of ξ is also limited by the instrument response function, which can be expressed in terms of a real-space window function through which the lattice is scanned [11.50]. With current instruments, the size of this window is roughly of the same size as L. Hence, recent improvements by orders of magnitude in the window width [11.43] may not be too helpful until better surfaces are available.

Local defects can be discussed in terms of their effect on the lattice gas Hamiltonian. If they create variations in the pair interactions, they couple to the energy density $|t|$. If α is nonnegative, they will beome important, with effects noticeable for $|t|$ less than of order $x^{1/\alpha}$, where x is the impurity concentration [11.51]. The transition may then be either

smeared or sharp but with crossover to a new set of exponents associated with the impure system. The crossover exponent is α. The unusually large values of α for the three- and four-state Potts models will produce unusually large t ranges in which the effects of defects should be observable. If defects modify the single-site energies, the effect is more severe. By causing a particular site to be occupied or vacant, they can produce shifts and rounding comparable to finite size effects. Moreoever, they can, by locally changing the stability of one sublattice versus the others, change the nature of the transition [11.52]. In fact, in a recent study of a random-field Ising model, they were found to destroy order [11.53]. Further discussion of defects and finite size appeared in a recent review [11.8]; an earlier review presented renormalization group results [11.54].

Very recent work combining finite size scaling and Monte Carlo has illustrated how a small impurity concentration can dramatically change critical exponents. In studying the Baxter-Wu model (three-spin interaction on a triangular lattice [11.4b]. NOVOTNY and LANDAU [11.55] found that a small concentration of quenched impurities (viz., randomly omitted spins) changed the exponents ν, γ, and α from four-state Potts values to 1.00 ± 0.07, 1.95 ± 0.08, and $\lesssim 0$, respectively, while producing no detectable change in β. The effect of defects on lattice systems is under active theoretical investigation. There is naturally the difficulty of drawing correspondences between the sorts of defects a theoretician can readily handle to the kinds encountered in real systems, but many of the effects are expected to be independent of details [11.53]. In some cases, the defects may even change the effective dimensionality, leading to apparent violations of the [hyper]scaling laws of (11.2) [11.53].

11.5 Case Study: O/Ni{111}

Considering the vast number of ordered chemisorbed patterns [11.32], one would expect to have little difficulty obtaining realizations of nearly all the entries in Table 11.1. Life is not so simple. In many cases, the substrates are {100} bcc faces, which have been found to undergo spontaneous reconstructions and thus do not provide a passive net of sites (for recent reviews and references see [11.56]). In other cases, the transitions turned out to be first order.

For the system c(2×2) Na on Ni{100}, the adlayer-induced spot intensity (vs T) was fit to the ONSAGER solution [11.3], although no attempt was made

to investigate exponents explicitly ([11.57], where a note added in proof raised the possibility that contaminants caused the order-disorder behavior). While such behavior is encouraging, a similar fit had been obtained earlier for c(2×2)H or D on W{100}[11.58], a complicated substrate as just noted. Better evidence is needed to confirm "simple" 2-d Ising behavior. Recently, the system c(2×2) O on Ni{100} was investigated [11.59]. Unfortunately, at the temperature at which the O disordered, it was found to dissolve into the bulk. For the system $(\sqrt{3} \times \sqrt{3})R30^{\circ}$ CO on Ru{0001}, a comparable problem arises: the CO desorbs as it disorders [11.60]. In either case these behaviors preclude the observation of critical scattering above T_c. It is not clear how these complications affect critical scattering below T_c, which in any case is very difficult to isolate. Perhaps eventually it will give some insight into the fluctuations which lead to disordering, but it is not a priori clear whether equilibrium is achievable or what is being held constant (not θ, maybe μ); these problems should not be tackled until more nearly ideal systems are well understood.

The remainder of this section will be devoted to work at Maryland, investigating the order-disorder transition of p(2×2) O on Ni{111} [11.19, 47,61,62]. This study is the first to extract critical exponents, 1) with LEED and also 2) for a chemisorption system. The phase diagram and adsorption sites were described in Chap.10. Once again, the subtle vertical displacements [11.63] of the three Ni nearest neighbors of each O do not remove the 2-d nature of the transition but merely rather passively alters the lateral interactions.

The experiments were carried out in a UHV bell jar at total base pressures below 10^{-10} torr. A quadrupole mass analyzer was used to monitor the composition of gases in the chamber. A standard four-grid LEED optics system was used for all other measurements. Thus the equipment is available in any modern surface physics laboratory. The Ni samples were 99.995% pure. They were zone refined to eliminate mosaic spread and oriented to the <111> direction to better than 20 min. Measurements could be made down to 100 K. With a thermocouple-driven feedback circuit controlling the sample heater, temperature stability of ±0.01 K was achieved. For further details of the apparatus and of sample preparation, see KORTAN and PARK [11.62].

A number of checks were performed to ascertain that the system was indeed on closed 2-d lattice gas. Monitoring the Auger peak height versus T showed that the oxygen did stay on the surface until 500 K [Ref.11.62, Fig.1]. At higher T it started to leave the surface; since no desorption was found, it must have dissolved into the bulk. To support the idea that

the oxygen adsorbed in the same kind of bonding state regardless of whether the overlayer was ordered, the adsorption-induced work function change $\Delta\phi$ (along with Auger intensity) were monitored versus exposure [Ref.11.62, Fig. 2]. Translated into $\Delta\phi$ versus coverage, one finds that $\Delta\phi$ increases linearly up to 1/4 monolayer, not being affected by the onset of order near 1/4 [Ref.11.62, Fig.3].

The hallmark of a second-order transition as observed in LEED was described in Sect.10.3.3 (also [Ref.11.62,Fig.4]). The intensity of the adlayer-induced spot drops off smoothly from a plateau as T increases. The width of the spot seems constant out to about the temperature at which the intensity reaches half its lowest value or has its point of inflection; then it increases rapidly with increasing temperatures. This broadening, due to critical scattering [cf. (11.20) and Fig.11.5], also occurs below T_c, but is overshadowed in a casual observation by the Laue scattering (broadened by the instrument). The first-order transition of the $(\sqrt{3} \times \sqrt{3})R30^\circ$ overlayer is strikingly different: the beam essentially disappears above the transition and the intensity plummets [Ref.11.62,Fig.5]. Moreover, an intensity -versus- T plot shows strong hysteresis [Ref.11.62,Fig.6]. Operationally, life is not so clear-cut. While some of the intensity above T_c in [Ref.11.62,Fig.4] is due to critical scattering, much or most comes from finite size effects of the substrate and the LEED instrument response. Apparent hysteresis can be produced at a second-order transition by cycling T so fast that equilibrium is not achieved; at first-order transitions the hysteresis can in principal be eliminated by extremely slow cycling. Finally, for low-coverage first-order transitions due to island dissolution, there is also apparent beam broadening with increasing T as the island size shrinks [11.64]. (Here, however, the drop in intensity T is greatly stretched out and different in shape [11.65]). These practical problems are reminiscent of similar difficulties in Monte Carlo described in Chap.10.

In this experiment, the beam intensity was monitored versus k along a cut through an adlayer-induced spot. This novel measurement was achieved by projecting a real image of the diffraction beam, via an optical system outside the vacuum chamber, onto the aperture (1°) of a photon counter. The sweep was achieved by varying the incident electron energy rather than the position of the detector. To minimize extraneous I-V variations, the incident energy at the spot center was picked to give a maximum in the I-V plot. A check [11.47b] indicated that these effects were well within our level of uncertainty. Sixty profiles were recorded between 323 and 450 K. Figure 11.6 illustrates early samples of such profiles, far noisier than used in the

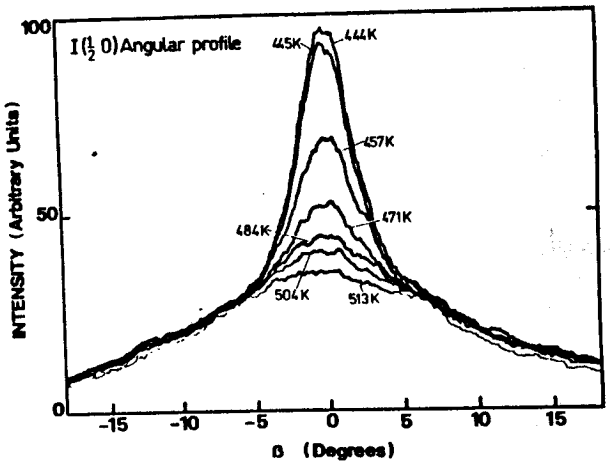

Fig.11.6. Angular profiles of an adlayer-induced LEED beam at several temperatures near T_c. Smoother versions of such profiles are the raw data for critical exponent analysis [11.61a]

analyses for exponents. Obviously the raw data are not very dramatic. In particular, it is hard to those locate T_c during the experiment. Preliminary processing included subtracting the uniform background due to thermal diffuse scattering and dividing out the effect of the Debye-Waller factor, as determined from the low-T dependence of the beam center.

The lowest T profile, more than 100 K below T_c, was used as the instrument response function. Two schemes were used to account for it. In the first, it was deconvoluted from the higher T profiles by dividing their 2-d Fourier transforms by its transform. From (11.20), we see that after this division the transformed profiles consist of a flat background proportional to $A|t|^{2\beta}$ and a peak at the origin (and at an array of real space points) with width proportional to ξ^{-2} and area proportional to χ. Operationally, there is much noise in the flat region due to uncertainty in the response function. The second approach, a fit scheme [11.66], takes advantage of (11.20) from the outset. That equation defines three temperature-dependent parameters which are determined (for each T) by convoluting with the instrument response function and optimizing the fit to the profile (at that T). Then each of these parameters are fit, again using a nonlinear least-squares routine, to the form of (11.3) where G(T) is the height of the delta-function contribution, the inverse amplitude of the Lorentzian (χ^{-1}), or the width of the Lorentziar the resulting exponents λ are 2β, γ, and ν, respectively. While (11.3) involves a three-parameter fit, it is sometimes desirable to set T_c and fit

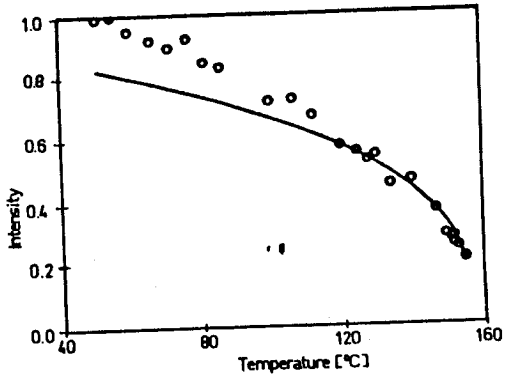

Fig.11.7. Analysis of the long-range-order intensity (at the center of the adlayer-induced beam) to determine the exponent β. The fitting range [120°C, 147°C] contains 7 data points [11.19]

just A and λ. The fitting scheme is the more expensive (time-consuming) method, but it is superior above T_c in that it avoids the persistent truncation oscillations of the first. Below T_c, the two methods give consistent results for β, while neither does well for the other two exponents because of noise after subtracting the long-range-order part. The choice of temperature range is important and nontrivial. The range should be as large as possible to enhance fitting statistics. It is limited at large $|t|$ by corrections to scaling and at small $|t|$ by finite size effects and incomplete deconvolution. In the present study, $0.015 \leq |t| \leq 0.06$ was used.

Plots of χ^{-1} [11.47a] and of width [11.47b] versus T for $T > T_c$ have already appeared in the literature. Both give T_c's slightly below 154°C. Due to overestimating T_c during the experiment (Fig.11.6), there were fewer data points below T_c. The analysis for β gave a T_c around 156°C. After reanalysis with T_c set at 154°C, β changed from 0.16 to 0.14, which seemed more trustworthy. Figure 11.7 illustrates this final analysis. We emphasize the sensitivity of the exponents to the value of T_c and hence the care that is required in the analysis (in an early crude analysis [11.47c], a T_c of 157°C was estimated and a β of 0.2 resulted).

A summary of the deduced exponents is presented in Table 11.2, along with the numbers for the Ising and the four-state Potts models. As noted in Chap.10, the expectation had been that the transition would fall into the four-state Potts universality class. This belief was based on the idea that the (2 × 2) pattern disordered into a triangular array of sites rather than a honeycomb array, i.e., into only one of the two kinds of three-fold sites. Monte Carlo results [11.19,47b] and fragmentary results on Heisenberg models with cubic anisotropy [11.67] suggested that the honeycomb cases exhibited only first-order transitions. The variety of complications discussed

Table 11.2. Exponent results, with model values for comparison (n.m.: not measured)

Exponent	Magnetic measurable	Ising	4-state potts	O/Ni{111} p(2 × 2)
α	Specific heat	0	2/3	n.m.
β	Magnetization	1/8	1/12	0.14 ± 0.02
γ	Susceptibility	7/4	7/6	1.9 ± 0.2
ν	Correlation length	1	2/3	0.94 ± 0.1

in Sect.11.2 were considered to try to understand the Ising-like exponents. The possibility of Fisher renormalization which would raise β, γ, ν by $(1 - \alpha)^{-1}$, i.e., by a factor of 3 for four-state Potts was dismissed because the coverage was 1/4, a symmetry value for which the line of constant chemical potential would have no kink at T_c in a T -versus- θ plot (cf. Fig.11.3 with Fig.10.12). The effect of logarithmic corrections [cf. (11.5)] were evaluated in the asymptotic limit ($|t| \to 0$), in which the constant term is neglected. This assumption was required since the data did not warrant a four-parameter nonlinear least-squares fit. Explicitly, effective exponents were predicted by optimizing fits of $|t|^{\lambda}$eff over the experimental thermal range to the form $|t|^{\lambda}(-\ln|t|)^{\tau}$, where τ = -1/3, 1/2, and 3/4 [11.21,68] for λ = 1/12, -2/3, and -7/6; the resulting λ_{eff}'s were 0.122, -0.80, and -1.37, respectively. All were thus substantially closer to the experimental numbers, but not by enough, particularly for γ. The effect of random surface defects or steps [11.69] might reduce the degrees of freedom for adatom fluctuations and thereby generate Ising-like behavior [11.70]. The work [11.55] on the impure Baxter-Wu model, cited at the end of Sect.11.4.2, found shifts of ν and γ to values consistent with the experimental results in Table 11.2. No corresponding shift of β could be detected. It is also not clear how such impurities would translate into the (2 × 2) lattice gas picture.

Another plausible explanation was suggested by SCHICK [11.71]. If E_0 is small [11.38], so that both kinds of three-fold sites are occupied, the (2 × 2) overlayer can be mapped into a Heisenberg model with cubic anisotropy, corners preferred. Each singly occupied cell of 8 sites in the overlayer goes into one site having a 3-d spin that can point to the 8 corners of a cube ($S_\alpha = \pm 1$ for $\alpha = x,y,z$). The four fcc or hcp sites go to the four corners having the same value of $S_xS_yS_z$ (i.e., ± 1); opposing vertices on the honeycomb go to (body-diagonally) opposing corners (Fig.11.8). This anisotropic Heisenberg system is a special case of the generalized Ashkin-Teller model studied very recently by GREST and WIDOM [11.72]; it contains a quadratic

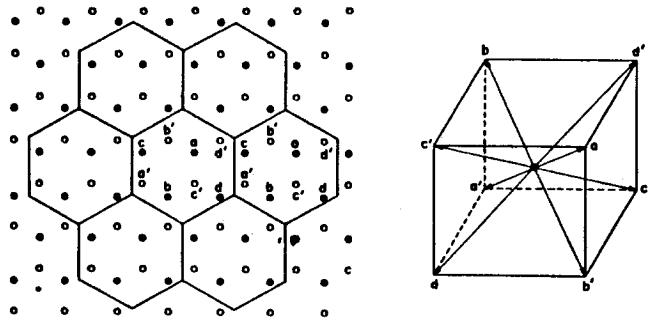

Fig.11.8. Correspondence between sites on a honeycomb lattice (with possible weak-energy differences between fcc and hcp sites) and the Heisenberg model with cubic anisotropy, corners preferred

term $K_2 \underline{S}_i \cdot \underline{S}_j$ plus a quartic term with coefficient K_4, both terms coupling nearest neighbors. For $K_4 = 0$, the three spin directions decouple, each having Ising character. This behavior persists for small negative K_4. For $K_4 > 0$, the model predicts first-order transitions. With a prefacing transformation ([11.36,73], in the latter identical results were obtained by matching the low-energy excitations of the two models), the lattice gas interactions can be related to K_2 and K_4. This model predicts that, if the experiment could go to smaller $|t|$, one would observe crossover behavior to the four-state Potts model with g proportional to E_0 and ϕ being 13/8 [11.71]. Very preliminary results do not support this viewpoint as the explanation [11.74].

11.6 Conclusions and Exhortations

While there has been dramatic progress during the last decade in both the theory of 2-d phase transitions and in surface physics, close interaction between the two has been a relatively recent occurrence, particularly in the case of chemisorbed atoms. In physisorption the lateral interactions are far better characterized, and graphitic surfaces enabled study by traditional diffraction probes. Recent work on a complicated puzzle provided by the chemisorbed overlayer O on Ni{111} suggests that complete characterization of such systems will require a large arsenal of techniques. It is particularly remarkable that a result from theoretical study of an abstract model was needed to provide the clue to obtaining a set of lateral interactions that adequately explain all qualitative features. In short, chemisorption

specialists cannot afford to be ignorant of new results in the theory of 2-d critical phenomena; correspondingly abstract theorists may find it gratifying to find that some models have realizations in the world, with complications that provide intriguing challenges.

For the 2-d statistical mechanic, many goals suggest themselves. Calculation of nonuniversal properties in terms of lattice gas parameters is crucial for a complete understanding of chemisorption systems. Detailed pictures of the correlation function, the size of critical region and the limiting corrections, and crossover behavior come readily to mind. The role of defects and finite plateaus also needs further attention; particularly important is some attempt to treat the actual defects, not just those that arise naturally in models.

Chemisorption experimentalists must identify more closed (no bulk absorption) systems and thoroughly characterize them. Critical exponents should be obtained at high- and low-symmetry regimes. Adlayer-induced spots should be examined above as well as below T_c. Efforts to probe smaller $|t|$ require both better LEED instruments (now becoming available) and better surfaces (a more difficult prospect). Close-packed surfaces should provide realizations of the three- and four-state Potts models [for {111} fcc or {0001} hcp faces] or the anisotropic XY model [for {110} bcc]. It would seem experience should be acquired on the former before tackling the less easily predictable latter. Also, a good $c(2 \times 2)$ layer on a square lattice would permit comparisons with the most tractable theoretical model.

An important role of the surface theorist is to promote meaningful communication between the two preceding groups. Another is to advance our understanding of the interactions between adatoms, and between defects and adatoms, from a solid-state or chemical vantage. Such knowledge is vital to simplify the parameter set with which one approaches 2-d simulation and to gauge whether the output is physically sensible.

It is "a magnificant thing to make clearer and clearer to oneself something that seemed at first to be ... totally confused [11.75].

Acknowledgments. Close collaboration with N.C. Bartelt, A. Refik Kortan, Robert L. Park, and particularly Lyle D. Roelofs is gratefully and happily acknowledged. The last's contributions can be gauged by the number of figures taken from his thesis, of citations of his papers, and of references drawn from Chap.10 and [11.19]. I also benefited from many informative and enjoyable conversations with J. Bhattacharjee, S. Fishman, J.F. Nicoll, and M. Schick. I am especially indebted to the last for a draft of his review article [11.9].

References

11.1 Y. Imry: In *Chemistry and Physics of Solid Surfaces II*, ed. by R. Vanselow (CRC, Boca Raton 1979) p.461; J.M. Kosterlitz: In *Phase Transitions in Surface Films*, ed. by G. Dash, J. Ruvalds (Plenum, New York 1980) p.193

11.2 B.I. Halperin, D.R. Nelson: Phys. Rev. Lett. *41*, 121, E515 (1978); D.R. Nelson, B.I. Halperin: Phys. Rev. B*19*, 2457 (1979)

11.3 L. Onsager: Phys. Rev. *65*, 117 (1944)

11.4a R.J. Baxter: J. Phys. A*13*, L61 (1980)

11.4b R.J. Baxter, F.Y. Wu: Phys. Rev. Lett. *31*, 1294 (1973); Aust. J. Phys. *27*, 357 (1974) R.J. Baxter: Phys. Rev. Lett. *26*, 832 (1971); Ann. Phys. N.Y. *70*, 193 (1972)

11.5a T.H. Berlin, M. Kac: Phys. Rev. *86*, 821 (1952)

11.5b H.E. Stanley: Phys. Rev. *176*, 718 (1968)

11.5c E. Helfand: Phys. Rev.*183*, 562 (1969)

11.6a J.G. Dash, J. Ruvalds (eds.): *Phase Transitions in Surface Films* (Plenum, New York 1980) [Proceeding of Nato Advanced Study Institute, Erice, June 11-25, 1979]

11.6b S.K. Sinha (ed.): *Ordering in Two Dimensions* (North Holland, New York 1980) [Proceedings of the International Conference, Lake Geneva, Wisconsin, May 28-30, 1980]

11.7 Phase Transitions on Surfaces, University of Maine, Orono, August 3-7, 1981; NATO Advanced Study Institute on Cooperative Phenomena in Two Dimensions, Banff, Summer, 1979

11.8 L.D. Roelofs: Appl. Surf. Sci. (to be published) [Proceedings of Second International Conference on Solid Films and Surfaces, College Park, Maryland, June 8-11, 1981]

11.9 M. Schick: Prog. Surf. Sci. (to be published)

11.10 C. Domb, M.S. Green (eds.): *Phase Transitions and Critical Phenomena* (Academic, London 1972-1976)

11.11 T.L. Einstein: In *Chemistry and Physics of Solid Surfaces II*, ed. by R. Vanselow (CRC, Boca Raton 1979) p.181

11.12 J.P. Muscat, D.M. Newns: Surf. Sci. *105*, 570 (1981); J.P. Muscat: J. Chem. Phys. (to be published)

11.13 V. Hartung: Z. Phys. B*32*, 307 (1979); J. Gallagher, R. Haydock: Surf. Sci. *83*, 117 (1979); G. Theodorou: Surf. Sci. *81*, 379 (1979); W. Kappus: Z. Phys. B*29*, 239 (1978); *38*, 263 (1980); J. Lopez, G. Allan: Surf. Sci. *103*, 456 (1981)

11.14 K. Binder, D.P. Landau: Surf. Sci. *61*, 577 (1976); Phys. Rev. B*21*, 1941 (1980)

11.15 H.E. Stanley: *Introduction to Phase Transitions and Critical Phenomena* (Oxford University Press, New York 1971)

11.16 S.-K. Ma: *Modern Theory of Critical Phenomena* (W.A. Benjamin, Reading, MA 1976)

11.17 F.J. Wegner: In Ref.11.10, Vol.6 (1976) p.124

11.18 A. Aharony, M.E. Fisher: Phys. Rev. Lett. *45*, 679 (1980)

11.19 L.D. Roelofs: Ph. D. Thesis, University of Maryland (1980)

11.20 M.E. Fisher, R.J. Burford: Phys. Rev. *156*, 583 (1967)

11.21 M. Nauenberg, D.J. Scalapino: Phys. Rev. Lett. *44*, 837 (1980); J.L. Cardy, M. Nauenberg, D.J. Scalapino: Phys. Rev. B*22*, 2560 (1980)

11.22 M.E. Fisher: Rev. Mod. Phys. *46*, 597 (1974) [and references therein]; E.K. Riedel, F.J. Wegner: Z. Phys. *225*, 195 (1969)

11.23 D.J. Amit, Y.Y. Goldschmidt, L. Peliti: Ann. Phys. N.Y. *116*, 1 (1978)

11.24a D.P. Landau, R.H. Swensen: Phys. Rev. Lett. *46*, 1437 (1981);

11.24b E.K. Riedel: Physica *106*A, 110 (1981) and references therein ;

11.24c A.N. Berker, S. Ostlund, F.A. Putnam: Phys. Rev. B*17*, 3650 (1978)

11.25 R.J. Birgeneau, G.S. Brown, P.M. Horn, D.E. Moncton, P.W. Stephens: J. Phys. C*14*, L49 (1981)

11.26 M.E. Fisher: Phys. Rev. *176*, 257 (1968)

11.27 A. Aharony: In Ref.11.10, Vol.6 (1976) p.357

11.28 G.Ya. Lyubarskii: *The Application of Group Theory in Physics* (Pergamon, Oxford 1960) Chap.7

11.29 D. Mukamel, S. Kransky: Phys. Rev. B*13*, 5065 (1976); C. Rottman: Phys. Rev. B*24*, 1482 (1981)

11.30a E. Domany, M. Schick, J.S. Walker: Phys. Rev. Lett. *38*, 1148 (1977);

11.30b E. Domany, M. Schick, J.S. Walker, R.B. Griffiths: Phys. Rev. B*18*, 2209 (1978);

11.30c E. Domany, M. Schick: Phys. Rev. B*20*, 3828 (1979)

11.31 S. Ostlund: Phys. Rev. B*23*, 2235 (1981)

11.32 G.A. Somorjai, F.Z. Szalkowski: J. Chem. Phys. *54*, 389 (1971); G.A. Somorjai, M.A. van Hove: *Adsorbed Monolayers on Solid Surfaces*, Structure and Bonding, Vol.38 (Springer, Berlin, Heidelberg, New York 1979)

11.33 J. José, L.P. Kadanoff, S. Kirkpatrick, D.R. Nelson: Phys. Rev. B*16*, 1217 (1977)

11.34 S. Alexander: Phys. Lett. A*54*, 353 (1975)

11.35 R.B. Potts: Proc. Cambridge Philos. Soc. *48*, 106 (1952)

11.36 A.N. Berker: Phys. Rev. B*12*, 2752 (1975); In Ref.11.6b, p.9

11.37 R.J. Baxter: J. Phys. C*6*, L445 (1973)

11.38 J.P. Hirth, J. Lothe: *Theory of Dislocations* (McGraw-Hill, New York 1968) pp.288ff, 764 [and references therein] W.A. Harrison: *Pseudopotentials in the Theory of Metals* (Benjamin, New York 1966) p.207

11.39 B. Nienhuis, E.K. Riedel, M. Schick: To be published

11.40 J.W. Essam: In Ref.11.10, Vol.2 (1972) p.197

11.41a P.W. Kasteleyn, C.M. Fortuin: J. Phys. Soc. Jpn. Suppl. *26*, 11 (1969);

11.41b C.M. Fortuin, P.W. Kasteleyn: Physica Utrecht *57*, 536 (1972);

11.41c A.B. Harris, T.C. Lubensky, W.K. Holcomb, C. Dasgupta: Phys. Rev. Lett. *35*, 327 (1975)

11.42 J. Als-Nielson: In Ref.11.10, Vol.5a (1976) p.87 H. Dachs (ed.): In *Neutron Diffraction*, Topics in Current Physics, Vol.6 (Springer, Berlin, Heidelberg, New York 1978) p.1

11.43 M. Henzler: Appl. Surf. Sci. (to be published); W.N. Unertl: Private communication

11.44 M.A. Van Hove, S.Y. Tong: *Surface Crystallography by LEED*. Theory, Computation and Structural Results. Springer Series in Chemical Physics, Vol.2 (Springer, Berlin, Heidelberg, New York 1979)

11.45 H.B. Tarko, M.E. Fisher: Phys. Rev. B*11*, 1217 (1975)

11.46 Robert L. Park: In *The Structure and Chemistry of Solid Surfaces*, ed. by G.A. Somorjai (Wiley, New York 1969) Chap.28

11.47a L.D. Roelofs, A.R. Kortan, T.L. Einstein, Robert L. Park: Phys. Rev. Lett. *46*, 1465 (1981)

11.47b L.D. Roelofs, A.R. Kortan, T.L. Einstein, Robert L. Park: J. Vac. Sci. Technol. *18*, 492 (1981)

11.47c L.D. Roelofs, A.R. Kortan, T.L. Einstein, Robert L. Park: In Ref. 11.6b, p.17

11.48 M. Fink, J. Ingram: At. Data *4*, 1 (1972); M.B. Webb, M.G. Lagally: Solid State Phys. *28*, 301 (1973)

11.49 Robert L. Park: Private communication

11.50 L.D. Roelofs, Robert L. Park, T.L. Einstein: J. Vac. Sci. Technol. *16*, 478 (1979)
11.51 A.B. Harris: J. Phys. C*7*, 1671 (1974);
A.B. Harris, T.C. Lubensky: Phys. Rev. Lett. *33*, 1540 (1974);
T.C. Lubensky: Phys. Rev. B*11*, 3573 (1975)
11.52 A. Aharony, Y. Imry, S.-K. Ma: Phys. Rev. Lett. *37*, 1364 (1976) [and references therein]
11.53 S. Fishman: Private communications;;
E. Pytte, Y. Imry, D. Mukamel: Phys. Rev. Lett. *46*, 1173 (1981) [and references therein]
11.54 A. Aharony: J. Magn. Magn. Mat. *7*, 198 (1978)
11.55 M.A. Novotny, D.P. Landau: Phys. Rev. B*24*, 1468 (1981)
11.56 P.J. Estrup: In *Chemistry and Physics of Solid Surfaces II*, ed. by R. Vanselow (CRC, Boca Raton 1979);
P.J. Estrup, R.A. Barker: In Ref.11.6b, p.39
11.57 S. Andersson: Nobel Symp. *24*, 188 (1973)
11.58 P.J. Estrup: In *The Structure and Chemistry of Solid Surfaces*, ed. by G.A. Somorjai (Wiley, New York 1969) Chap.19
11.59 D.E. Taylor, Robert L. Park: Appl. Surf. Sci. (to be published) [Abstract]
11.60 D. Menzel: Private communication
11.61a A. Refik Kortan: Ph. D. Thesis, University of Maryland (1980)
11.61b A.R. Kortan, P.I. Cohen, R.L. Park: J. Vac. Sci. Technol. *16*, 541 (1979)
11.62 A.R. Kortan, Robert L. Park: Phys. Rev. B*23*, 6340 (1981)
11.63 T. Narusawa, W.M. Gibson, E. Törnqvist: Phys. Rev. Lett. *47*, 417 (1981)
11.64 J.C. Buchholz, M.G. Lagally: Phys. Rev. Lett. *35*, 442 (1975)
11.65 M.G. Lagally, G.-C. Wang, T.-M. Lu: In *Chemistry and Physics of Solid Surfaces II*, ed. by R. Vanselow (CRC, Boca Raton 1979) p.153
11.66 J. Als-Nielsen, O.W. Dietrich: Phys. Rev. *153*, 706 (1967)
11.67 M. Schick: Private communication
11.68 J. Bhattacharjee, D.J. Scalapino: Private communication
11.69 P. Kleban: Surf. Sci. *103*, 542 (1981);
P. Kleban, R. Flagg: Surf. Sci. *103*, 552 (1981)
11.70 J. Nicoll: Private communication
11.71 M. Schick: Phys. Rev. Lett. *47*, 1347 (1981)
11.72 G. Grest, M. Widom: Phys. Rev. B*24*, 6508 (1981)
11.73 N.C. Bartelt, T.L. Einstein: Unpublished
11.74 L.D. Roelofs, N.C. Bartelt, T.L. Einstein: Phys. Rev. Lett. *47*, 1348 (1981)
11.75 P. Ehrenfest to H.A. Lorentz, 1 January 1924, cited by M.J. Klein: Physica *106*A, 3 (1981)

Note added in proof:

I.F. Lyuksyutov, A.G. Fedorus: Sov. Phys. JETP *53*, 1317 (1981) [Zh. Eksp. Teor. Fiz. *80*, 2511 (1981)], recently reported the critical exponent β, obtained via LEED, for the disordering of the (2×1) and of the (2×2) overlayers of H chemisorbed on W{110}. Their analysis procedure is less sophisticated than that in Sect.11.5. These transitions lie in the class with non-universal exponents.